Estimating impedance from PP and PS seismic data at the Ross Lake oilfield, Saskatchewan

Chuandong (Richard) Xu and Robert R. Stewart

ABSTRACT

A 3C-3D surface seismic data was acquired over Husky Energy Inc.'s Ross Lake heavy-oil field in southwestern Saskatchewan. In a previous interpretation, a V_p/V_s map between the Index Horizon Above Cantuar Marker (IHACM) and the RushLake horizon was calculated by combining PP and PS traveltime-thickness maps. In this paper, the impedance inversions are performed on the poststack PP and PS data using STRATA and ProMC. Dividing the average of the inverted P-impedance over an 8-ms horizon-based time window by the average of the inverted S-impedance over the same window, we map the V_p/V_s with higher vertical resolution. The V_p/V_s value derived from impedance inversion is generally lower than the V_p/V_s derived from the time-thickness ratios. The impedance V_p/V_s and traveltime V_p/V_s values show promising anomalies.

INTRODUCTION

Husky Energy's Ross Lake heavy-oil field is located in southwestern Saskatchewan. Sand bodies of incised-valley channel systems, or possibly shore deposits, have developed in proximity to the Dimmock Creek member of the Cantuar formation of the Mannville Group in the Lower Cretaceous. These oil-saturated sands are the drilling targets.

A 3-D multicomponent seismic survey was conducted over this area by Veritas DGC in 2002. Veritas also processed the 3C-3D data from field edits through poststack migrations of the vertical-, radial-, and transverse-component volumes. Based on the vertical (denoted as PP) and radial (denoted as PS) migrated results, a preliminary interpretation has been offered by Xu and Stewart (2003). In that paper, a promising V_p/V_s map (Figure 1) was developed that was interpreted as being a sand indicator. This map was created by combining PP and PS time-thickness maps calculated between the IHACM and RushLake horizons that include the reservoir interval. This sand indicator map from the V_p/V_s value has been correlated with results from a horizontal well log (Figure 1).

In this paper, we employ a widely used seismic inversion package, STRATA, to invert the poststack PP and PS volumes into impedance traces. We arrive at a V_p/V_s map by dividing the inverted P-impedance by the inverted S-impedance.

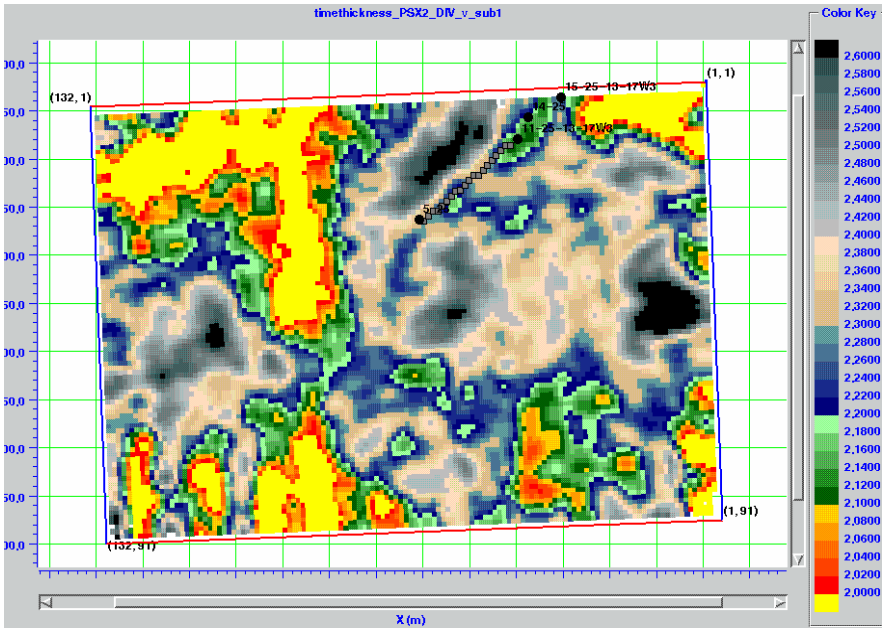

FIG. 1. Map of average V_p/V_s between the IHACM and RushLake horizons (from Xu and Stewart, 2003). We interpret the yellow and green areas as sands, while the black and grey areas are more shaly.

PP DATA INVERSION

Before designing the background velocity model for the inversion, the correlation between the well logs and the well-site seismic trace is carefully checked using synthetic seismogram. A small stretch of the logs is performed.

The east-west seismic line (crossline) 11, which crosses well 11-25 in the northern section of the 3D, is used as a reference line in the following inversions. By default, all profiles shown here are for crossline 11. Well 11-25 has the requisite logs. The P-impedance is derived by multiplying the measured P-velocity log and the density log. To extend the P-impedance trace to the entire 3-D area, four picked seismic horizons — the Viking, IHACM, RushLake and GravelBourg, respectively — are used to constrain the horizontal interpolation of the impedance log. Then, a 20-Hz low-pass filter is applied to arrive at the low-frequency trend (Figure 2) that acts as the P-impedance model.

The P wavelet is next extracted from all the PP seismic traces excluding the edge traces. Then, a model-based inversion is performed to invert the PP seismic traces into P-impedance traces. Figure 3 shows one east-west crossline which crosses well 11-25. Notice that the inversion does find a low P-impedance area at the target zone.

We calculate an average P impedance, using an 8-ms window centred 14 ms above the RushLake horizon. In plan view (Figure 4), we can see the low-impedance anomaly associated with the reservoir sand body.

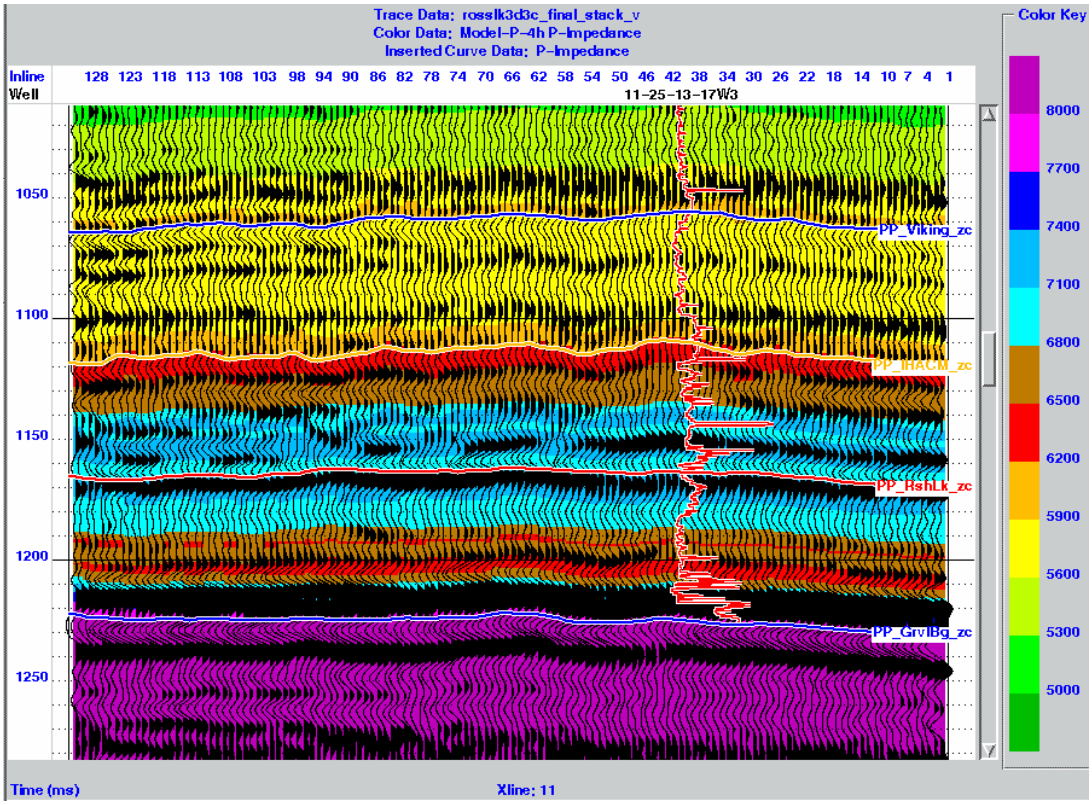

FIG. 2. The background P-impedance model with P-impedance log inserted at the well location.

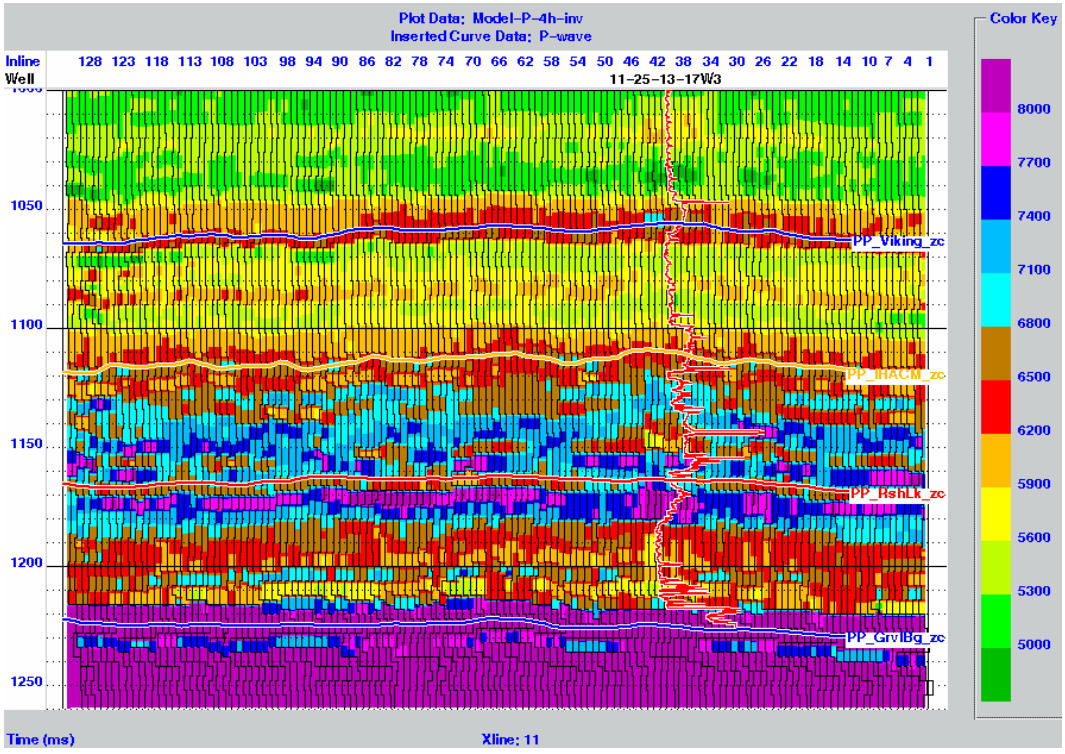

FIG. 3. Results of the model-based P-impedance inversion.

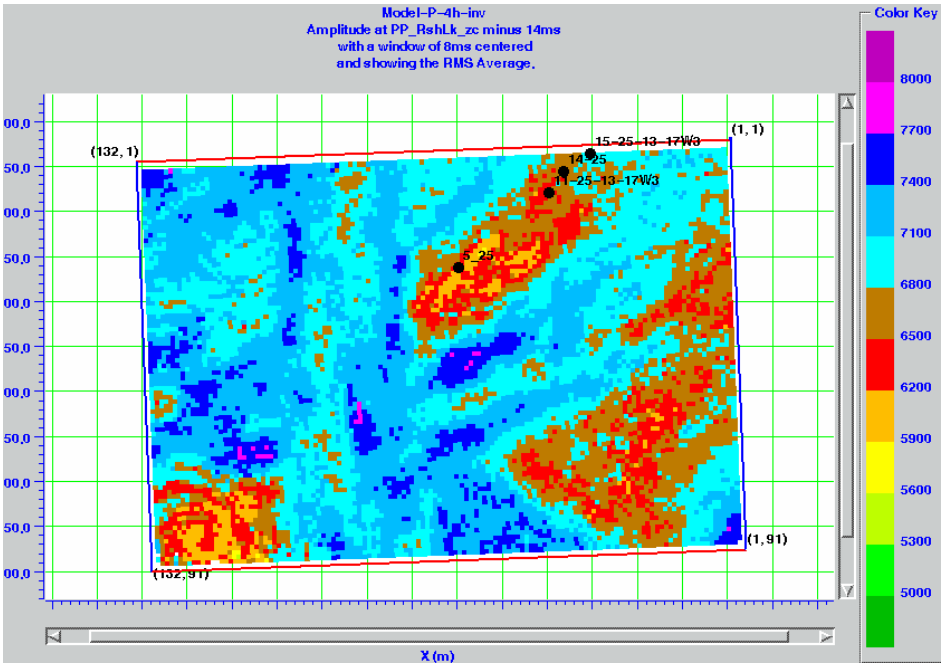

FIG. 4. The average impedance over an 8-ms window centred at 14 ms above the RushLake horizon.

PS DATA INVERSION

To accomplish the PS inversion, we make the simplifying and quite approximate assumption that the PS reflectivity is linearly proportional to the SS reflectivity. In reality, the relationship is more complex and is dependent on the trace offsets comprising the stacked PS seismogram, as well as the time-dependent incidence angle. Nonetheless, relative changes in the PS reflectivity over small depths may be highlighted by the approximate inversion procedure.

PS to PP horizon matching

ProMC, a multicomponent seismic-data interpretation package, is used for registering PP and PS events. The previous interpretation work revealed an event correlation between PP and PS data, by integrating well logs and offset-VSPs. Figure 5 displays the PP and PS seismic data of crossline 11 in PP time. We have annotated four picked events. The PS-to-PP time conversion is accomplished using a fixed V_p/V_s value of 2.35.

In the process of horizon matching, all four PS horizons are forced to match the same horizons in PP time. Therefore, the V_p/V_s of each trace between those events are obtained by this traveltime-adjustment (Figure 6). Note that the colour on the PS data panel has changed from a constant shade (before matching) to one with variation (after event matching).

After horizon matching, the PS data in PP time are exported from ProMC, and then imported into STRATA.

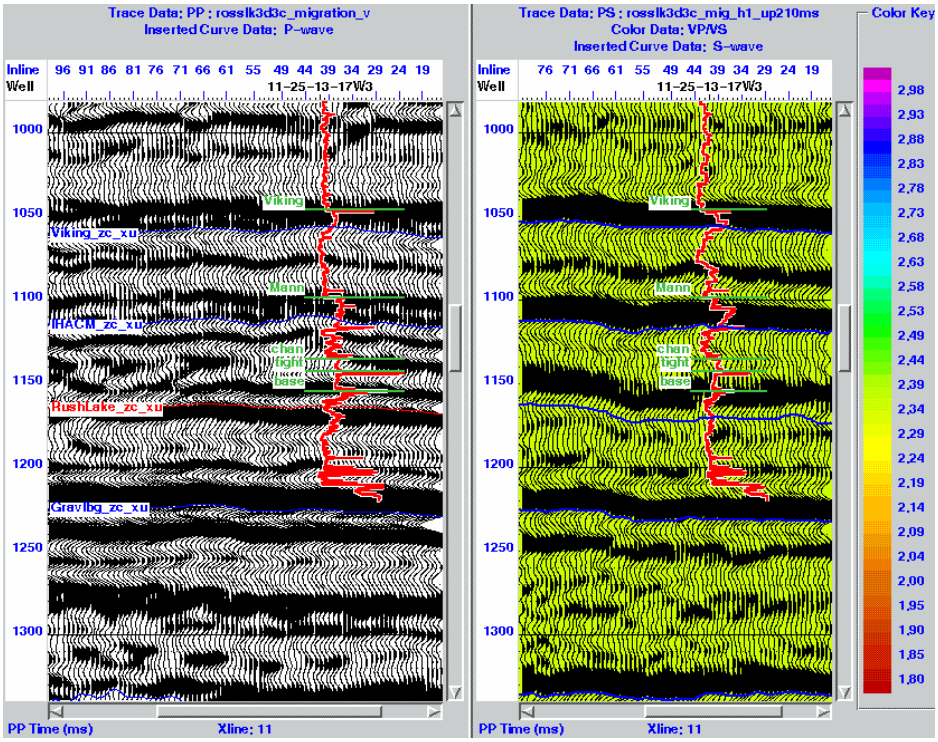

FIG. 5. PP (left) and PS data (right) seismic sections in PP time using a constant V_p/V_s=2.35.

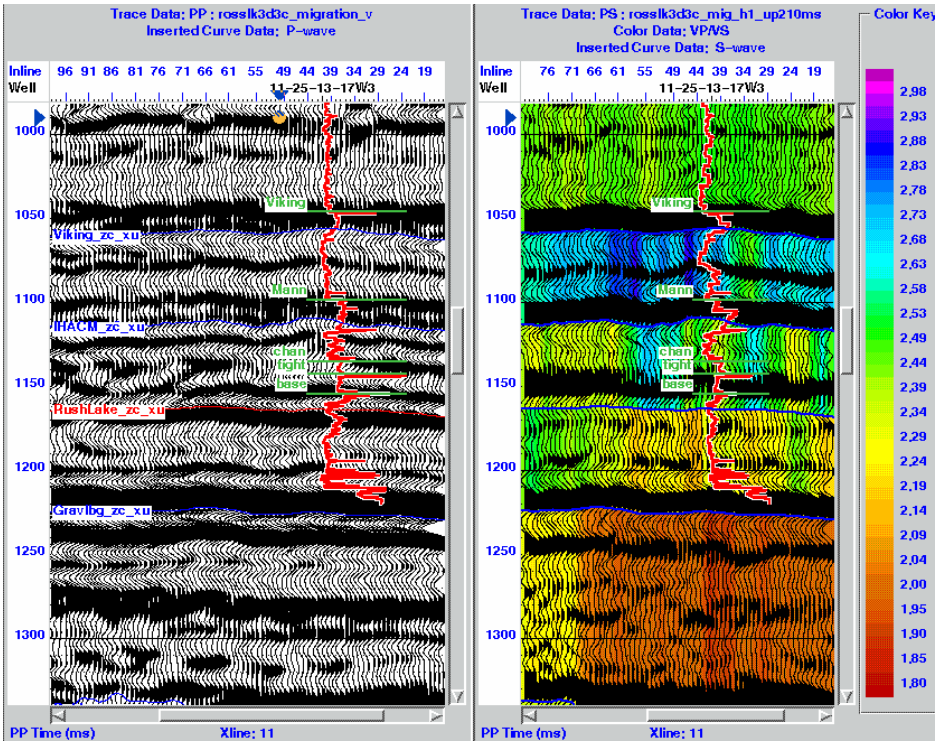

FIG. 6. After horizon-matching: Notice the colour changes that indicate the V_p/V_s values used in the matching.

Build S-impedance model

The PS data are now in the PP time at the four picked horizons, which means the same set of picked events in PP time that are used to create P-impedance mode should be used to create the S-impedance model. The difference is that S-impedance model trace value comes from multiplying the S-velocity log and density log. Then, a low-pass filter is applied to the model to keep the initial model smooth (Figure 7).

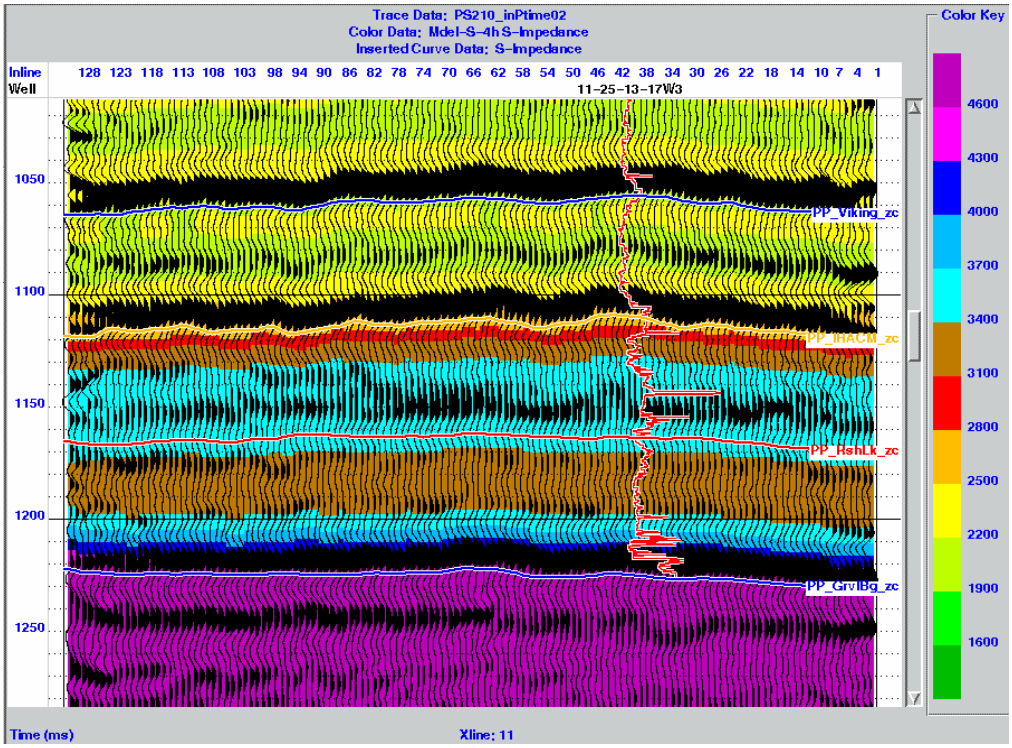

FIG. 7. The S-impedance background model.

The next step is to use the well-modelling module to check the correlation between the PS synthetic log and PS seismic trace, and stretch or squeeze the logs if needed. The wavelet is then statistically extracted from all the PP-time PS seismic traces, excluding the edge traces, in the 800–1300 ms time window, assuming zero-phase.

Inversion

Two inversion techniques are investigated here: model-based and sparse-spike. In this case, there is no directly measured shear-wave log for well 11-25. So, the shear-velocity is derived using the first-arrival time picked from the vertical-source and horizontal-source zero-offset VSP traces to get an interval V_p/V_s, which is then multiplied by the measured P-velocity to get the S-velocity. Therefore, this S-impedance model may not be perfectly correct. We found that the sparse-spike inversion seems to be less noisy than model-based inversion. We chose the sparse-spike inversion result as our final result (Figure 8).

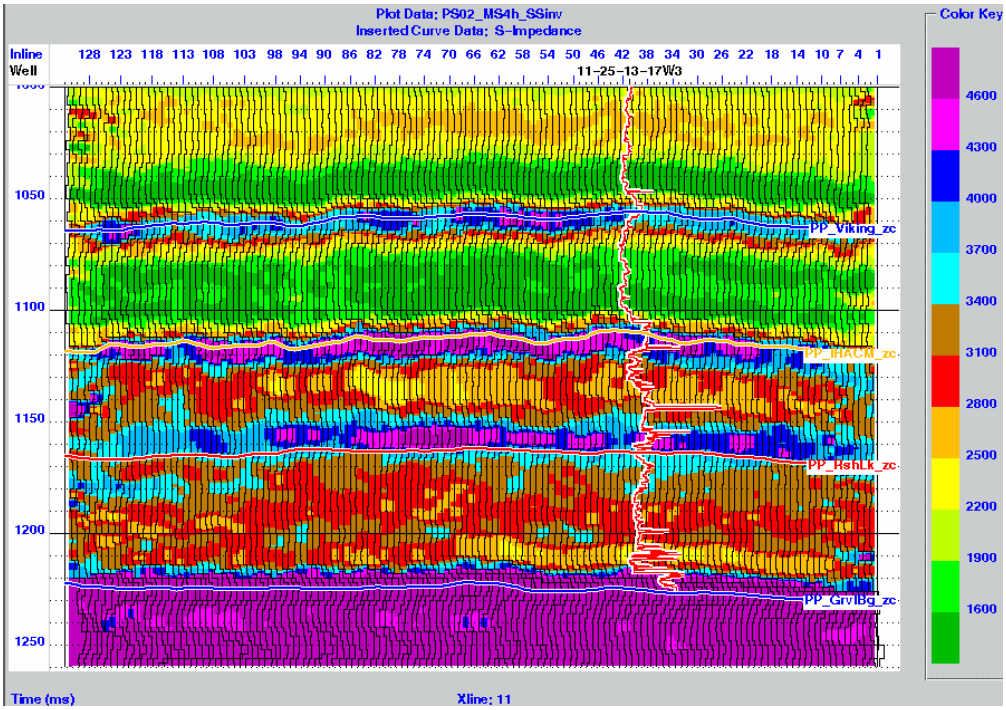

FIG. 8. The inversion result of PS data, east-west crossline 11.

V_P/V_S CALCULATION

Now we have two 3-D volumes of the inverted P-impedance and S-impedance. Ideally, the V_p/V_s volume can be derived by dividing the P-impedance by the S-impedance. However, the PP and PS time registration remains as a problem: by horizon matching, we only force PS time equal to PP time along the four horizons. All the time-points between horizons do not necessarily correspond until we have a very accurate V_p/V_s at each spatial point and at each sampled time — which is what we want to achieve.

Therefore, an average value over a certain time window is perhaps more reasonable. By checking the horizon slices of the inverted P-impedance, rising from the RushLake horizon in 4-ms increments, we notice that an 8-ms window centred 14 ms above the RushLake horizon is a relatively good-sized window, which is used to get the RMS average of the P-impedance. The upper-left map in Figure 9 shows this average which we interpret to represent the target zone. The sand body is featured with low P-impedance value.

The RMS average of inverted S-impedance is also calculated in the same 8-ms window centred 14 ms above the RushLake horizon (Figure 9, right map).

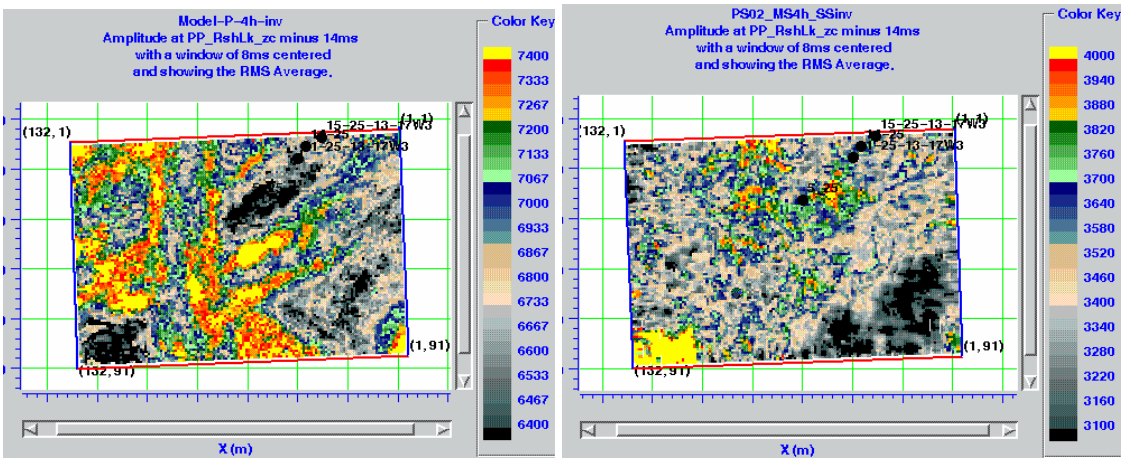

FIG. 9. Average P-impedance (left) over an 8-ms window indicates the sand has a low P-impedance value (dark color) while the average S-impedance (right) shows a high S-impedance value.

Then, the V_p/V_s map is manipulated by dividing the average P-impedance by the average S-impedance. A comparison of the impedance-derived V_p/V_s and traveltime-derived V_p/V_s is shown in Figure 10. Bear in mind that, using the impedance method, the V_p/V_s is an average over an 8-ms (PP time) window, meanwhile, the V_p/V_s from traveltime is an average over a 40~50-ms (PP time) window.

Some observations from these two V_p/V_s maps are:

1. Overall, the impedance-derived V_p/V_s map has a lower V_p/V_s value, which ranges from 1.5~2.3 with reservoir sand about 1.6~1.7, than the traveltime V_p/V_s, which ranges from 1.7~2.6 with reservoir sand about 2.15~2.25.

2. The low-V_p/V_s strip on the left of the traveltime V_p/V_s map disappears on the impedance V_p/V_s map.

3. The size of the sand body looks more extensive in area on the impedance V_p/V_s map.

4. The sand body has an eastern direction extension on both impedance V_p/V_s and traveltime V_p/V_s maps.

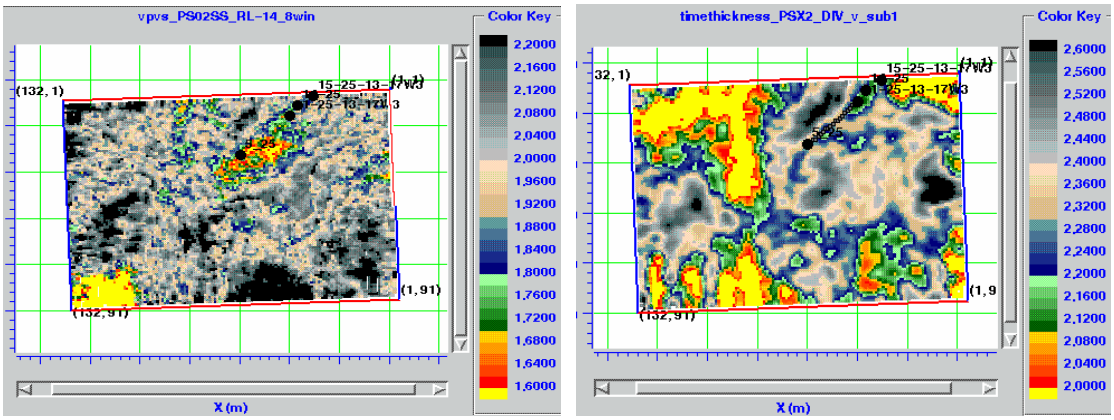

FIG. 10. Comparison of V_p/V_s derived from impedance (left) and V_p/V_s derived from time-thickness ratios (right).

DISCUSSION

Inversion is a data-driven process. When we look at the data (Figure 6), above the IHACM and below the RushLake horizon, the PP and PS data are correlated in terms of their seismic characters. Between these two horizons, where the zone of interest lies, the PP data show several events. In contrast, PS section has only one wide, low-frequency, low-amplitude peak. This difference is sufficient to create the discrepancy between PP and PS inversion. Figure 11 is the analysis of PP and PS inversion at the well location. The arrow indicates the zone of interest, which is between the IHACM and RushLake horizons.

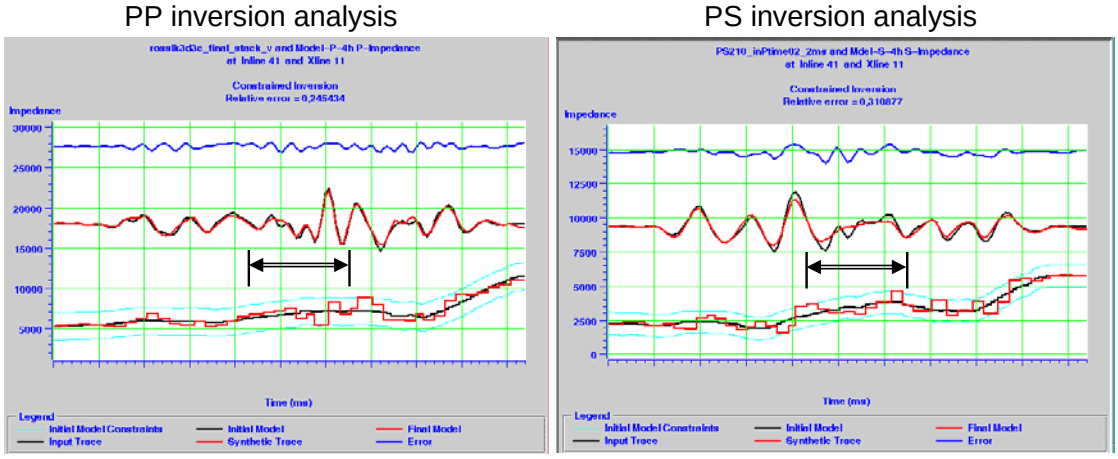

FIG. 11. Inversion analysis of PP (left) and PS (right) trace at the well location. The arrow indicates the interval between IHACM and RushLake. X-axis is time, moving deeper to the right.

At the well location, in the zone of interest, the PP seismic trace shows a good correlation with PP synthetic. However, the PS seismic trace doesn't show such a good correlation with the PS synthetic seismogram (Figure 12). We hope to improve the imaging and frequency content in future, interpretive-oriented, PS-data reprocessing.

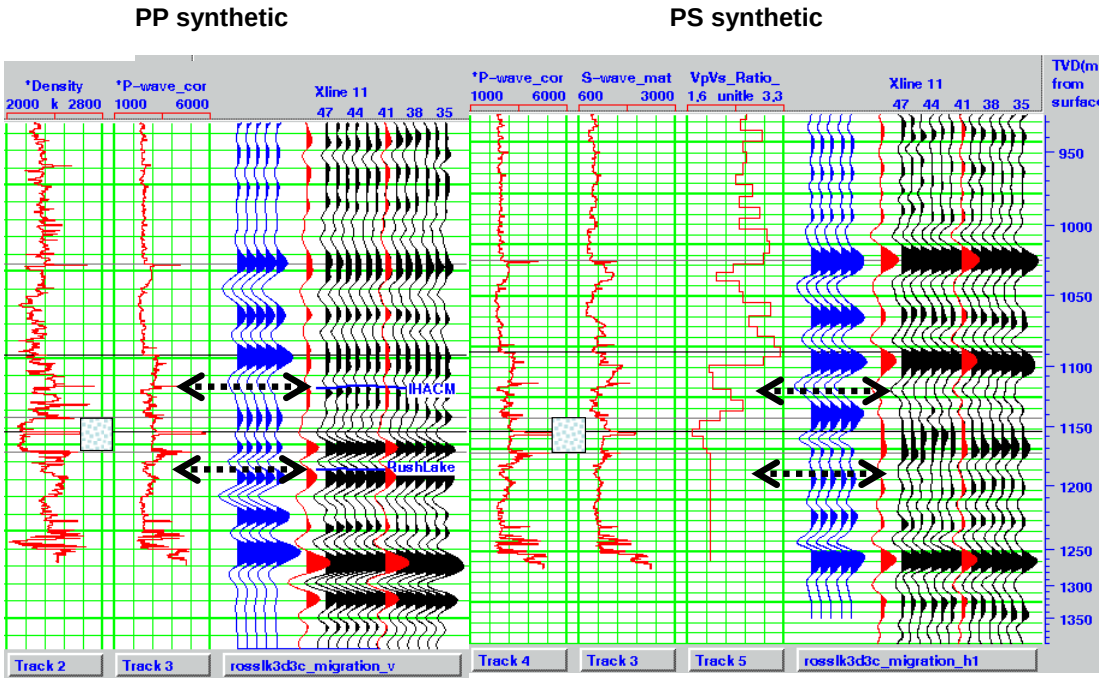

FIG. 12. PP and PS synthetic seismograms and seismic traces.

CONCLUSION

The PP data-inversion indicates that the oil-bearing sand body has a lower P-impedance compared with surrounding formation. In contrast, PS data inversion shows the sand has a slightly higher S-impedance. The V_p/V_s value derived from impedance inversion is generally lower than the V_p/V_s derived from the time-thickness ratios. The impedance V_p/V_s and traveltime V_p/V_s values show promising anomalies.

ACKNOWLEDGEMENTS

We would like to thank Husky Energy Inc. for providing the 3C-3D seismic data and Hampson-Russell Software Services for donating STRATA and ProMC. We also thank all sponsors for their support of CREWES.

REFERENCES

Xu, C., and Stewart, R. R., 2003, Ross Lake 3C-3D seismic survey and VSP, Saskatchewan: a preliminary interpretation: CREWES Research Report, **15**.